JOURNAL OF MATERIALS SCIENCE 29 (1994) 255–261

Structure and growth of platelets in graphite spherulites in cast iron

BAIHE MIAO*, D. O. NORTH WOOD
Department of Mechanical Engineering, University of Windsor, Windsor, Ontario, Canada
WEIMIN BIAN
Materials Analysis Centre, North east University of Technology, Shenyang 110006, People's Republic of China
KEMING FANG, MINZ HENG FAN‡
*Department of Physical Chemistry,‡ Department of Mechanical Engineering , * and also Department of Materials Science and Engineering, University of Science and Technology Beijing, Beijing 100083, People's Republic of China*

The structure and orientation of graphite platelets in graphite spherulites (GS) in cast irons modified by either cerium or magnesium plus cerium were investigated by TEM and micro-diffraction. The platelets have a rhombohedral structure with their [0 0 1] directions nearly parallel to the radius of the GS, but each platelet is twisted about 2° over a 1 μm length. Randomly orientated graphite is located in the interplatelet areas, in which most of the graphite has a hexagonal structure rather than rhombohedral structure. Based on the crystallographic characterization of the graphite and the cerium and magnesium elemental distribution in the GS, the model for the growth of GS as originally proposed by Double and Hellawell is re-examined.

1. Introduction

In previous studies of microstructure and growth of graphite spherulites (GS) in nodular cast irons which had been modified by magnesium and/or cerium, there have been many reports of the structure, hexagonal or rhombohedral, and growth mechanisms for these spherulites [1–6]. In their study, Double and Hellawell [1] claimed that the crystal structure of all forms of graphite present, including the fine eutectic flakes, the very fine semi-fibrous graphite and the nodular graphite, was hexagonal with open hexagonal rings stacked in an ABAB, . . . , sequence and with an axial ratio $(c/a) = 2.73$. Lux *et al.* [2] and other researchers [3–5] also reported the graphite structure to be hexagonal.

In the cast irons and natural graphite, crystallographic defects such as stacking faults, intercalation, twins, various tilt and rotation boundaries, have been observed to be present in the graphite structure [3,7]. High-resolution electron micrograph (HREM) lattice fringe images of graphite platelets have also revealed the existence of dislocations, branching and bending of the platelets and intercalary layers of CeS_2 and Ce_2O_2S in the graphite spherulites [8].

With respect to the growth mechanism of the graphite in the spherulites, Double and Hellawell [1,4] first proposed a cone–helix model for the growth of the spherulites. By examination of the growth structure, they were able to explain some of the structural characteristics of the spherulites, though their model at that stage lacked experimental confirmation. Subsequently, Chen *et al.* [9] in their SEM study of the morphologies of a large number of sections of the graphite spherulites etched with ion sputtering, found that the sections consisted of cone–helixes, thus supporting Double and Hellawell's model. However, features such as the orientation of the *c*-axis and the precise growth mechanism of the graphite basal plane layers in the spherulites, were unclear due to the lack of sufficient supporting experimental evidence, such as that obtained from diffraction, TEM and HREM observations. Given this lack of experimental evidence, the method of growth of the graphite basal planes, as in Double and Hellawell's model, is not yet fully understood. Also, the effects of cerium and magnesium additions on the nucleation and growth of the graphite, as well as on the formation of graphite spherulites, were not fully described in these earlier papers.

This investigation was to examine the crystallographic structure and orientations of the graphite platelets and interplatelet areas in a fan-like area of graphite spherulites in cast irons which had been modified by cerium or magnesium, using TEM and micro-diffraction techniques. Based on this information, a growth model for the platelets and the graphite spherulites in cast irons is described in detail.

2. Experimental procedure

The chemical compositions of the cast irons used in this study are given in Table I. Cast iron A was

0022–2461

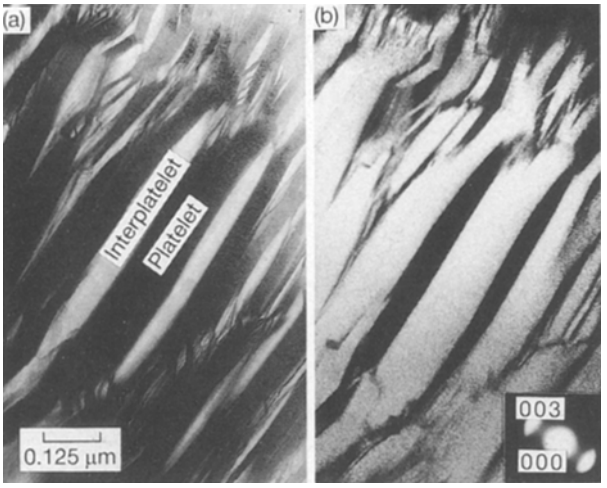

Figure 1 Microstructure of platelets in a fan-like area of a GS. (a) Bright field image. (b) g 0 0 3C dark-field image and its SAD patterns. The fan-like area is consisted of well-developed graphite platelets which are nearly parallel oriented, and interplatelet areas.

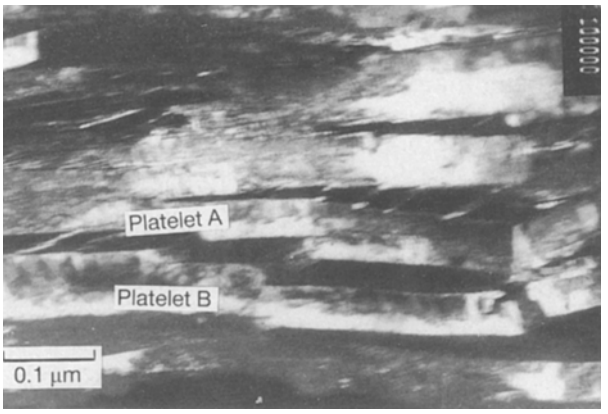

modified by cerium only and was melted in a carbon-tube furnace under an argon atmosphere. Cast iron B is a pilot-plant cast iron modified with both magnesium and cerium and was produced by electron slag melting.

The preparation process for their foil specimens of the graphite spherulites is described in detail elsewhere [8]. The crystallographic structure and orientation of graphite were determined by SAD and by taking micro-diffraction patterns along the longitudinal platelets at 50 nm intervals in a fan-like area of a graphite spherulite. A Phillips EM-400T transmission electron microscope was used in this study. The compositions of the inclusions in the graphite spherulites were determined by EDS techniques in a Hitachi-800 TEM.

3. Results and discussion

The microstructure of a fan-like area of a GS is shown in Fig. 1. The platelets have similar crystallographic orientations but there are interplatelet areas.

Two series of micro-diffraction patterns for the graphite [0 1 0] zone axis with a rhombohedral structure taken from points along a platelet from left to right at intervals of 50 nm, are shown in Fig. 2. In order to show the extent of the orientation change in a platelet, we have placed the zone axis centre of every diffraction

Figure 2 Two series of micro-diffraction patterns of the [0 1 0] zone axis from rhombohedral structure graphite taken along each platelet at 50 nm intervals. The bright field image is also given. The zone axis centre of every diffraction photograph is on the same line in order to show the orientation changes within a platelet. t, spots from twin reflections.

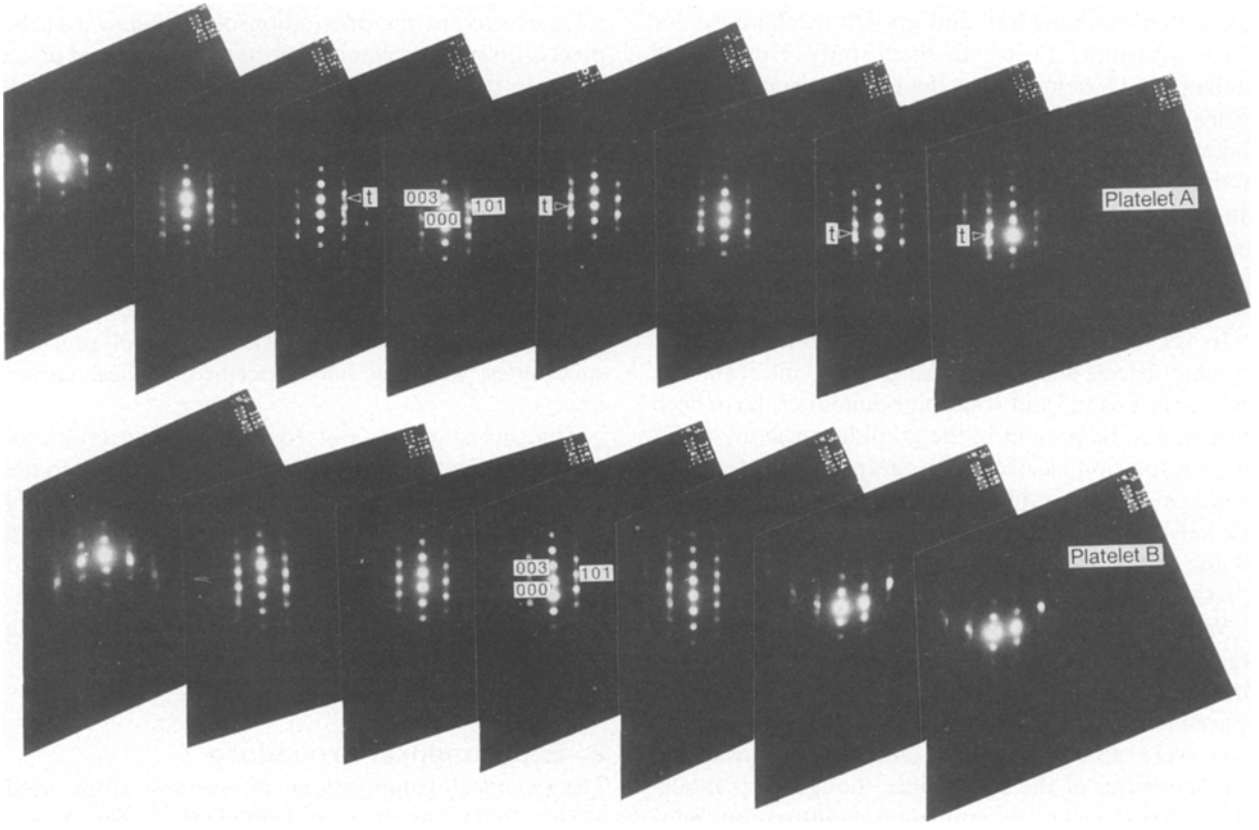

pattern on the same straight line. The orientation change is calculated using the Bragg equation $2d\sin\Theta = \lambda$, where Θ is the Bragg reflection angle (deg) (here it is the tilt angle of crystal as measured by the deviation from the zone axis centre), d the distance of the transmitted spot from the zone axis centre in each micro-diffraction pattern (nm); λ the electron wavelength, 0.0037 nm at 100 kV, The orientation changes thus measured in the two platelets (A and B) in a fan-like area shown in Fig. 2, are summarized in Table II.

Fig. 3 shows another set of micro-diffraction patterns, and their indexing, which were taken at 50 nm intervals along two interplatelet areas, A and B, which were situated on either side of a platelet. From these diffraction patterns, it is deduced that most of the graphite in the interplatelet areas has the hexagonal structure but with varying (random) orientations.

Fig. 4 shows the cerium and sulphur elemental EDX spectrum in a section of the graphite spherulite. The inclusions (black in the micrograph) at the centre of the spherulite are high in cerium and sulphur content. The concentrations of cerium and sulphur decrease on going from the centre to the outside of the spherulite.

TABLE I Chemical compositions of cast irons (wt %)

	C	Si	P	S	Mn	Ce	Mg	Fe
A	4.2	1.07	0.005	0.003	0.19	0.32	–	bal.
B	2.51	3.28	0.080	0.0018	0.54	0.0024	0.016	bal.

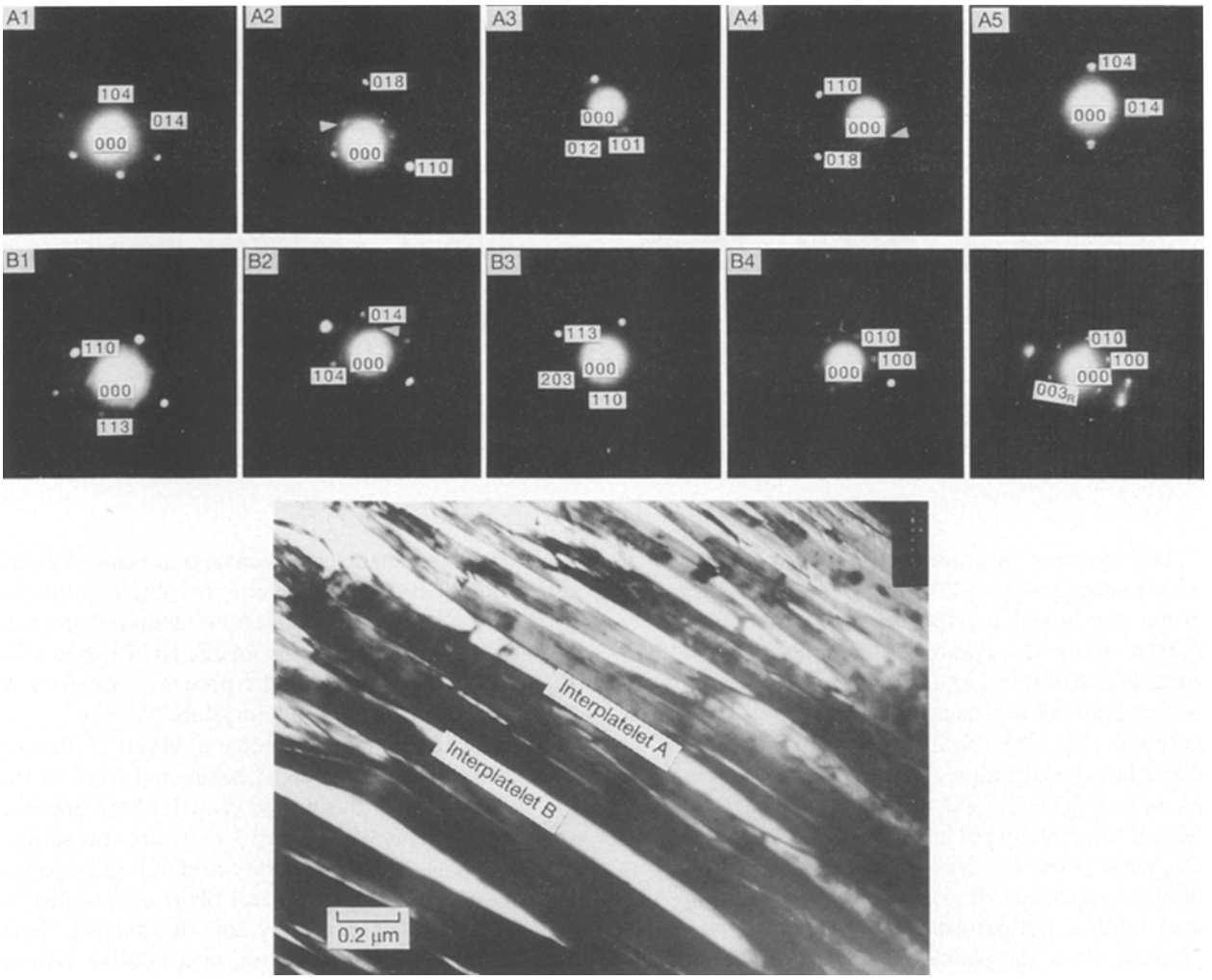

Figure 3 Micro-diffraction patterns of $[4\,4\,1]_R$, $[0\,8\,1]_R$, $[1\,2\,1]_R$, $[8\,8\,1]_R$, $[4\,4\,1]_R$ and $[3\,3\,2]_{HEX}$, $[4\,4\,1]_R$, $[3\,3\,2]_{HEX}$, $[0\,0\,1]_{HEX}$ from left to right and then from top to bottom every 50 nm apart from two interplatelet areas situated on both sides of a platelet respectively. Also shown is the bright-field image. The last pattern is a complex SAD pattern for $[0\,0\,1]_{HEX}$ which comes from interplatelet and $[0\,1\,0]_R$ platelet, respectively. The extra spots marked with an arrow in the corresponding patterns come from other orientations of graphite.

TABLE II The [001] orientation changes of graphite within a platelet relative to the symmetrical axis of the cone

Platelet	Position							
	1	2	3	4	5	6	7	8
A	− 0.95°	− 0.25°	− 0.1°	0°	0°	+ 0.05°	+ 0.63°	+ 0.95°
B	− 1.0°	− 0.5°	− 0.1°	+ 0.05°	+ 0.1°	+ 0.9°	+ 1.25°	–

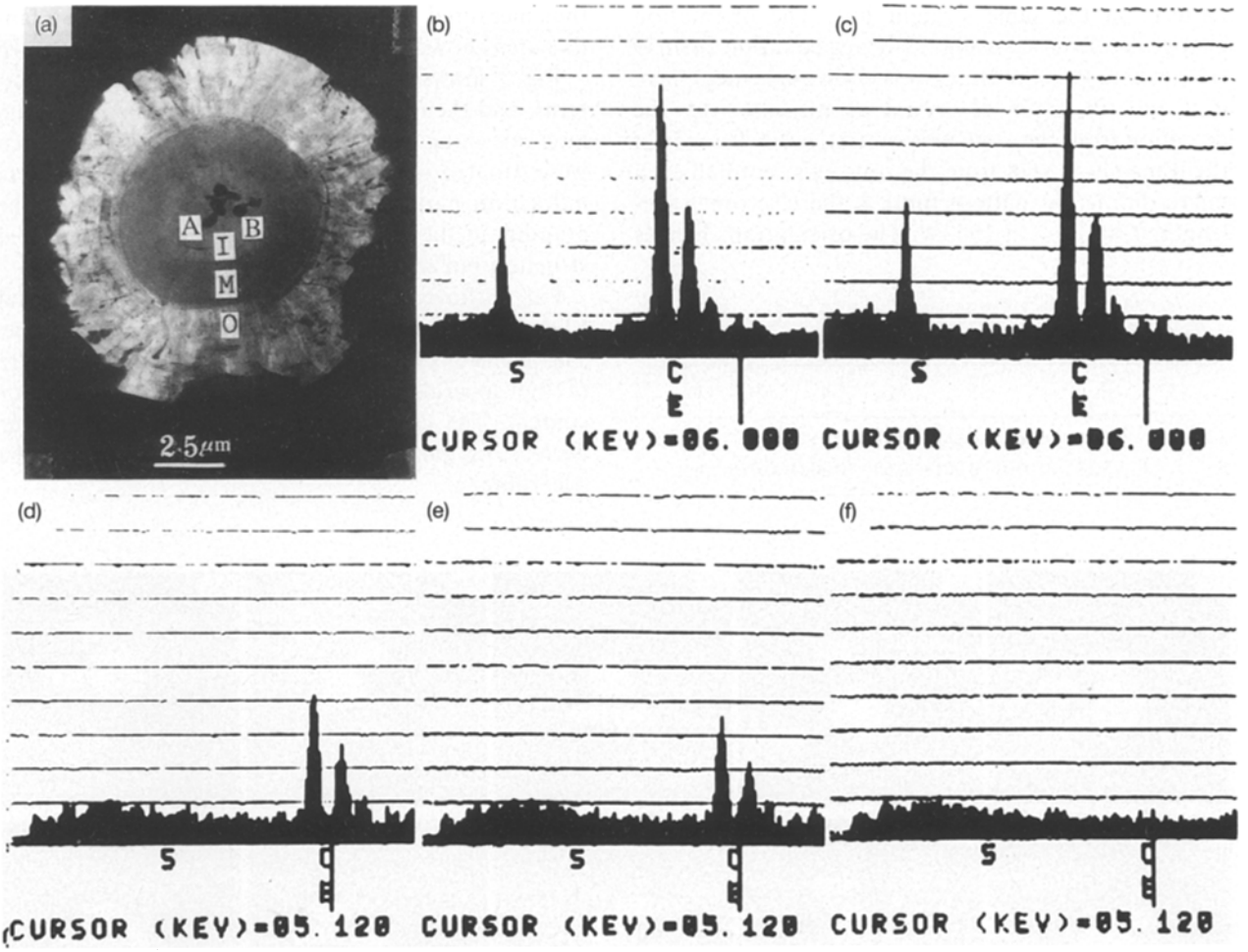

Figure 4 The microstructure of a graphite spherulite in a cerium-doped iron, and the cerium and sulphur elemental EDX spectrum in this section of the spherulite. (a) The microstructure of a section of a graphite spherulite with several nuclei. (b, c) The cerium and sulphur elemental EDX spectrum in particles A and B in the graphite spherulite. (d–f) The cerium and sulphur elemental EDX spectrum in the different areas of the section, marked I, M and O, as shown in (a).

The structure of graphite can be either hexagonal with a space group of $P6_3/mmc$ [6], where the carbon atoms are linked together in sheets that are widely spaced along the c-axis, or rhombohedral, with a space group of $R\bar{3}m$ [6] or R3 [10]. The two structures of the graphite are usually referred to as 2H or 3R graphite [6]. The rhombohedral lattice as indexed using hexagonal indexes obeys the rule $-h + k + l = 3n$ ($n = 0, \pm 1, \pm 2, \pm 3, \ldots$) for lattice extinction. If the structure is hexagonal, with a space group $P6_3/mmc$, when $1 = 2n + 1$ and $h = k$, there are forbidden reflections due to structure extinction. The micro-diffraction patterns for the [0 1 0] zone axis of graphite show the platelets to have a rhombohedral structure rather than hexagonal structure (see Fig. 2). It is impossible to differentiate between the $R\bar{3}m$ or R3 space groups of graphite by analysis of the [0 1 0] zone axis patterns. However, based on the extinction rule for the reflected planes and the geometric distributions of the [0 0 1] zone axis pattern, it is not difficult to confirm that the structure of the platelets in the graphite spherulites is rhombohedral rather than hexagonal. The randomly orientated graphite in the interplatelet areas, in which most of the graphite has a hexagonal rather than rhombohedral structure (see Fig. 3), may have resulted from the graphite formed behind the platelets, which had grown from different directions. An attempt was made using convergent beam electron diffraction (CBED) experiments to obtain more information on the graphite but no structural detail was found in the CBED patterns for the [0 1 0] zone axis. This was probably due to the presence of defects in this direction in the graphite crystals.

The [0 0 1] orientation change of about 2° along a platelet means that the basal hexagonal rings of the platelet are twisted during the growth of the graphite spherulite. This is why the 0 0 3 spots are spread into an arc (see Fig. 1). The graphite could thus grow by the bending and branching of basal plane as revealed by HREM lattice fringe images and the platelets have about a 10° spread orientation in a fan-like area of GS [8].

From the observations on the morphologies and microstructure of graphite spherulites, as well as the crystallographic structure and orientation changes of platelets, we deduce that the platelets are the skeleton or primary structural unit and that each fan-like area, i.e. the aggregate of similarly oriented platelets, is the secondary structural unit, a cone–helix of a graphite spherulite. It has been previously assumed that there could be three forms of graphite growth in a spiral mechanism: as seen in Fig. 5a, b and c [1]. However, an aggregate formed from platelets is not a real conical helix but a cone–helix type cylinder [1, 4], as shown in

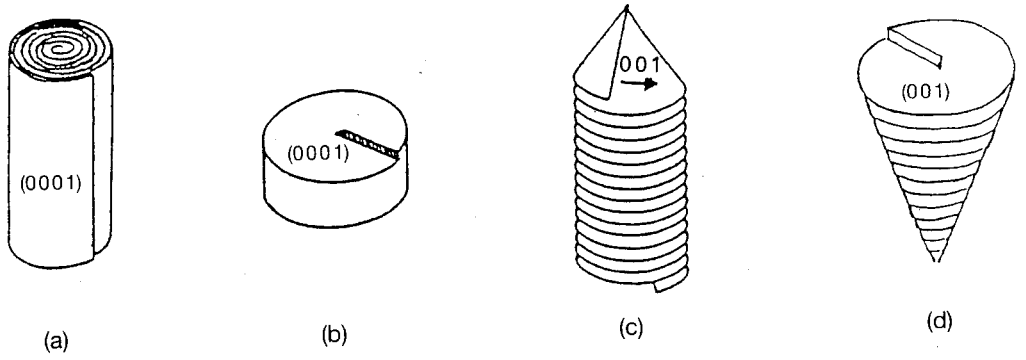

Figure 5 Basal scroll forms of graphite growth. (a) The classical screw terrace with $\alpha = 180°$, like a roll of carpet. (b) A conical helix with the basal scroll $\alpha = 0°$. (c) A cone–helix type cylinder. (d) A sketch of a single conical helix.

Fig. 5c. The {0 0 1} planes of graphite which are rotated around the cone symmetric axis, have a dip angle related to the axis in Double and Hellawell's model [1, 4], see Fig. 4c. In this case, the [0 0 1] direction of graphite would not be parallel to the symmetric axis of the cone–helix even if it is parallel to the electron beam.

Based upon the present results and Double and Hellawell's model, it is suggested that a graphite spherulite consists of conical helixes which grow out of the graphite platelets. A single conical helix with various sections through the cone is shown in Fig. 6. The {0 0 1} planes of graphite within each conical helix grew up around the symmetric axis of the cone and ⟨0 0 1⟩ direction of graphite is nearly parallel to the axis; see Figs 5d and 6.

The existence of crystallographic defects in the graphite crystals could influence their growth. For instance, twins can lead to bending of the crystal out of the basal plane while stacking faults may lead to branching of the crystal within the basal plane. Screw dislocations and intercalation may provide the steps in spiral growth [11]. In addition, the existence of the interplatelet areas in the spherulites has shown that the predominant platelets which grow in the spiral are not perfect in structure.

In this study, no microstructural differences were found for graphite spherulites in cast irons modified by either cerium or magnesium plus cerium, except the inclusions in the core of the GS.

Cerium together with sulphur and oxygen are able to form inclusions of Ce_2O_2S and Ce_2O_3 in cerium-doped cast irons. Most of the inclusions are removed in the slag, but those remaining in the melt can act as heterogeneous nuclei for the graphite. It has been shown that most graphite spherulites in cerium-treated cast irons have a cerium-rich nucleus, as shown in Fig. 4. Magnesium additions produce a different effect and no magnesium-rich inclusions in graphite spherulites were found. However, in the sections of a GS, there are two to three areas where the cerium content is decreasing from the centre to the periphery, see Fig. 4. It should be pointed out that these results are from the areas where no significant inclusions containing cerium, i.e. Ce_2O_2S or Ce_2O_3, were found.

With regard to the nucleation of the graphite spherulites which have grown in a spiral, it may be instructive to consider the possible role played by the C60 structure [12, 13], where the carbon atoms are balled into a cluster, like a football which is a polyhedron with 60 vertices and 32 faces, 12 of which are pentagonal and 20 hexagonal. The C60 structure with a diameter of 0.7 nm approximates a spherical shell of graphite and provides an inner cavity, in which a variety of atoms may be held. Recently, a C60La structure was discovered [14], in which the lanthanum makes C60La stable. That may also be the basic role played by the addition of cerium, lanthanum and magnesium as spheroidization agents. The C60 polyhedron may also act as a common nucleus of the conical helixes in a GS, and keep the graphite continually growing along the planes on the surface of polyhedron by a spiral mechanism.

Before concluding this discussion, we would like to outline our picture of the growth of the graphite spherulites. It is assumed that the tiny crystals of cerium oxysulphide or a C60 structure provide the 'base' for the nucleation and growth of the platelets of graphite which are themselves the basic structural units (skeleton) of the graphite cone. The apexes of the cones are 'rooted' on the facets of the oxysulphide crystals and C60 structure which have a polyhedral shape. The cones grow radially from the nucleus while the platelets spread out spirally around the axis of each cone. Each platelet is slightly twisted around the conical axis. While the platelets grow out spirally, and are twisted in a continuous and smooth fashion, there is bending, and branching, and intercalations and dislocations are formed. Consequently, the interplatelet areas are formed behind the platelets in the graphite spherulite of the cast iron.

4. Conclusions

1. Graphite platelets with a rhombohedral structure as the 'skeleton' for the graphite spherulites.

2. Randomly orientated graphite is located in interplatelet areas and most of the graphite has a hexagonal structure.

3. The [0 0 1] direction of each platelet is twisted about 2° around the radius of the graphite spherulite and the ⟨0 0 1⟩ directions of all platelets are orientated nearly parallel to the radius. These suggest that the graphite has grown in a spiral manner from a common nucleus. The nucleus could be either a cerium-rich

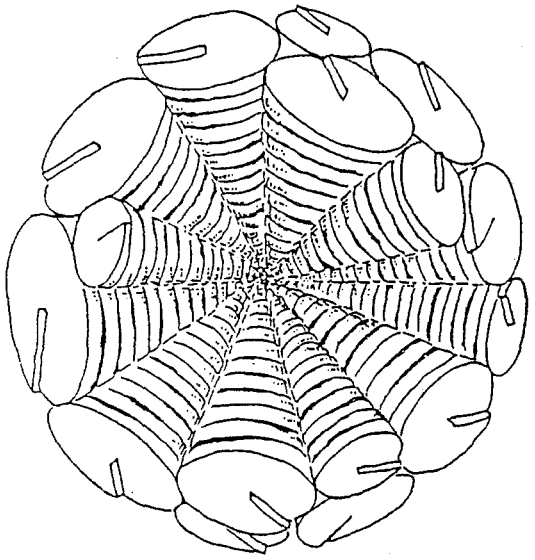

(a)

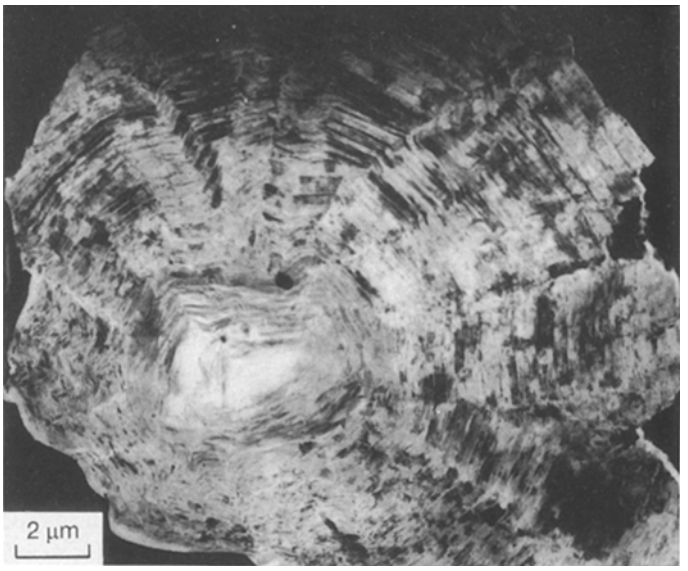

(b)

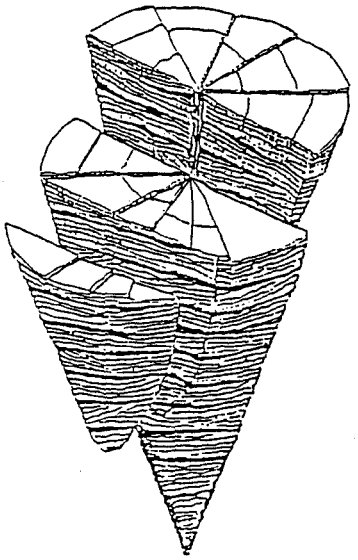

(c)

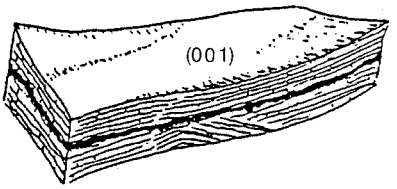

(d)

Figure 6 A structure model of a GS, with improvements shown to Double and Hellawell's cone–helix model. (a) Schematic structure model of a GS. (b) Microstructure of a section of a GS. (c) A single conical helix with various sections. (d) Schematic diagram of twisted growing platelets with inter platelets.

inclusion for cerium-modified irons or a C60-like polyhedron for magnesium-doped irons.

4. The existence of interplatelet areas and crystallographic defects in graphite spherulites, may be a result of intergrowth of the graphite platelets.

5. Some modification of Double and Hellawell's model of GS is proposed, whereby fan-like aggregates of platelets in a GS are real reciprocal cones, i.e. conical helixes topped by the centre of the GS. This modified model, leads to a better understanding of the growth morphologies, microstructure and crystallographic characterization of the graphite in graphite spherulites in the cast irons.

Acknowledgements

The authors thank Professor Gongdu Zhou, Beijing University, for stimulating discussions. This research was supported by the Agency of Rare-earth Metals of the Ministry of the Metallurgical Industry and the University of Science and Technology Beijing.

References

1. D.D. DOUBLE and A. HELLAWELL, in "The Metallurgy of Cast Iron", edited by B. Lux, I. Minkoff and F. Mollard, (Georgi, St Saphorin, Switzerland, 1975) p. 509.
2. B. LUX, I. MINKOFF, F. MOLLARD and E. THURY, *ibid.*, p. 495.
3. J. P. SADOCHA and J. E. GRUZLESKI, *ibid.*, p.443.
4. D. D. DOUBLE and A. HELLAWELL, *Acta Metall.* **22** (1974) 481.
5. I, MINKOFF, "The Physical Metallurgy of Cast Irons", (Wiley-Interscience, New York, 1983) p. 108.
6. L. G. BERRY and B. MASON, "Mineralogy", 2nd Edn (Freeman, San Francisco, 1983) p. 245.
7. F. HUBBARD HORN, *Nature* 4 October (1952) 581.

8. BAIHE MIAO, KEMING FANG, WEIMING BIAN and GUOXUN LIU, *Acta Metall. Mater.* **38** (1990) 2167.
9. CHEN SYCEN *et al.*, *Acta Mech. Engg.* **18** (1982) 7 (in Chinese).
10. Joint Committee Powder Diffraction Standards (JCPDS) File No. 26-1079 (JCPDS, Swarthmore, PA, 1976).
11. M. HILLERT and Y. LINDBLOM, *JISI* (April) **192** (1954) 388.
12. A. D. J. HAYMET, *J. Am. Chem. Soc* **108** (1986) 319.
13. H. W. KROTO, J. R. HEATH, S. C. O'BRIEN, R. F. CURL and R. E. SMALLEY, *Nature* **318** 14 November (1985) 162.
14. J. R. HEATH, S. C. O'BRIEN, Q. ZHANG, Y. LIU, R. F. CURL, H. W. KROTO, F. K. TITTEL and R. E. SMALLEY, *J. Am. Chem. Soc.* **107** (1985) 7779.

Received 25 March 1993
and accepted 2 June 1993